ACS Sustainable Chemistry & Engineering

pubs.acs.org/journal/ascecg

Research Article

Carbon-Electrode-Mediated Electrochemical Synthesis of Hypervalent Iodine Reagents Using Water as the O-Atom Source

Scott J. Folkman,* Richard G. Finke, José Ramón Galán-Mascarós, and Garret M. Miyake*

Cite This: *ACS Sustainable Chem. Eng.* 2021, 9, 10453−10467

Read Online

ACCESS | Metrics & More | Article Recommendations | Supporting Information

ABSTRACT: Photoelectrocatalytic water splitting is an important goal of modern chemistry that is hindered by the slow kinetics of anodic water oxidation. Additionally, the O_2 byproduct of water oxidation catalysis is of little economic value. One way to increase the energy efficiency as well as economic feasibility of photoelectrocatalytic water splitting as an industrial process is to couple the oxidation of water to the formation of value-added, oxygenated products such as olefin epoxidation or other selective oxygenation or oxidation reactions—rather than the coupling of two O-atom equivalents to O_2. However, attempts at direct olefin epoxidation at the same anode where water oxidation catalysis is happening suffer from competing one-electron oxidation or overoxidation of the olefin substrate. Hence, an O-atom-transfer mediator is needed. Hypervalent iodine reagents are known to perform olefin epoxidations via O-atom transfer, oxidation reactions, as well as a myriad of other group-transfer reactions. A drawback addressed in the following work is that the synthesis of hypervalent iodine reagents typically requires the use of a powerful oxidant such as IO_4^- or $KHSO_5$ with multiple steps and potentially explosive intermediates or side products. Herein, we report proof-of-principle electrochemical syntheses of a series of hypervalent iodine reagents, including: λ^3-*o*-iodosobenzoic acid (IBA) in up to 58% isolated yield with a Faradaic efficiency 89%; the previously inaccessible λ^3-ethyl 2-iodosobenzoate (IBA-ester) with ∼78% Faradaic efficiency; the well-known λ^5-2-iodoxyphenyl *tert*-butyl sulfone (IBX-sulfone) with ∼51% Faradaic efficiency; and a mixture of λ^3-2-iodosobenzene sulfonic acid (IBA-sulfonic acid) with λ^5-2-iodoxybenzene sulfonic acid (IBX-sulfonic acid) with an overall Faradaic efficiency of >78%. Mechanistic studies using $H_2{}^{18}O$ in the electrochemical synthesis demonstrate that the O-atom in the product is initially transferred from the oxidized, O-atom-containing surface of the glassy carbon electrode, with ^{18}O from $H_2{}^{18}O$ then replacing the O-atom vacancy on the carbon electrode surface. Overall, the present contribution demonstrates the electrochemical, green synthesis of novel and well-known hypervalent iodine reagents using the O-atom from H_2O. The reported studies also provide insights into the electrochemical mechanism needed to optimize the synthesis yields as well as to exploit those syntheses using O-atom equivalents generated via (photo)electrochemical water splitting.

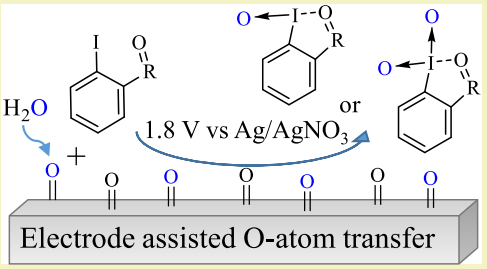

KEYWORDS: *catalysis, oxygenation, electrosynthesis, green synthesis, group transfer, epoxidation, oxidation, electrochemical mediators*

INTRODUCTION

Photoelectrocatalytic water splitting is an important if not critical goal of modern chemistry.[1] However, the kinetic bottleneck of water splitting is the anodic oxidation of water, a $4e^-/4H^+$ process and yields O_2 as a product of little economic value. We and others[2−6] hypothesize that water oxidation could be coupled to other chemical processes to yield value-added products. Attempts to do direct oxygenation of organic substrates anodically often lead to overoxidation or $1e^-$ chemistry forming unwanted byproducts—necessitating the use of an electrocatalytic mediator.[2,4,7] An important recent example using an electrocatalytic mediator is the anodic epoxidation of ethylene to ethylene oxide mediated by Cl/ClO^-.[7] The use of chloride as a mediator for O-atom transfer is a convenient and simple method but is limited to a Faradaic efficiency of ∼70% even after optimization at 300 mA/cm^2 with ethylene oxide production rate at ∼170 mg/h[7] and, critically, the Cl/ClO^- couple lacks synthetic tunability by electronic or steric modifications as is possible in organic-based systems.

Alternatively, hypervalent iodine reagents such as λ^3-iodosobenzene (PhIO) or λ^5-*o*-iodoxybenzoic acid (IBX) and their derivatives are known to perform O-atom-transfer oxygenation reactions including olefin epoxidation, alcohol oxidation, and alkane hydroxylation in the presence of a transition-metal catalyst.[8−11] Furthermore, the λ^3-iodine species *o*-iodosobenzoic acid (IBA) can perform oxygenation of α,β-unsaturated ketones when converted to the *n*-tetrabutylammonium salt,[12] is selective toward peptide

Received: February 24, 2021
Revised: April 7, 2021
Published: July 23, 2021

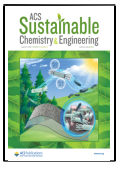

Scheme 1. Structure, Equivalent Valency, and Abbreviations of Hypervalent Iodine Reagents Used Herein

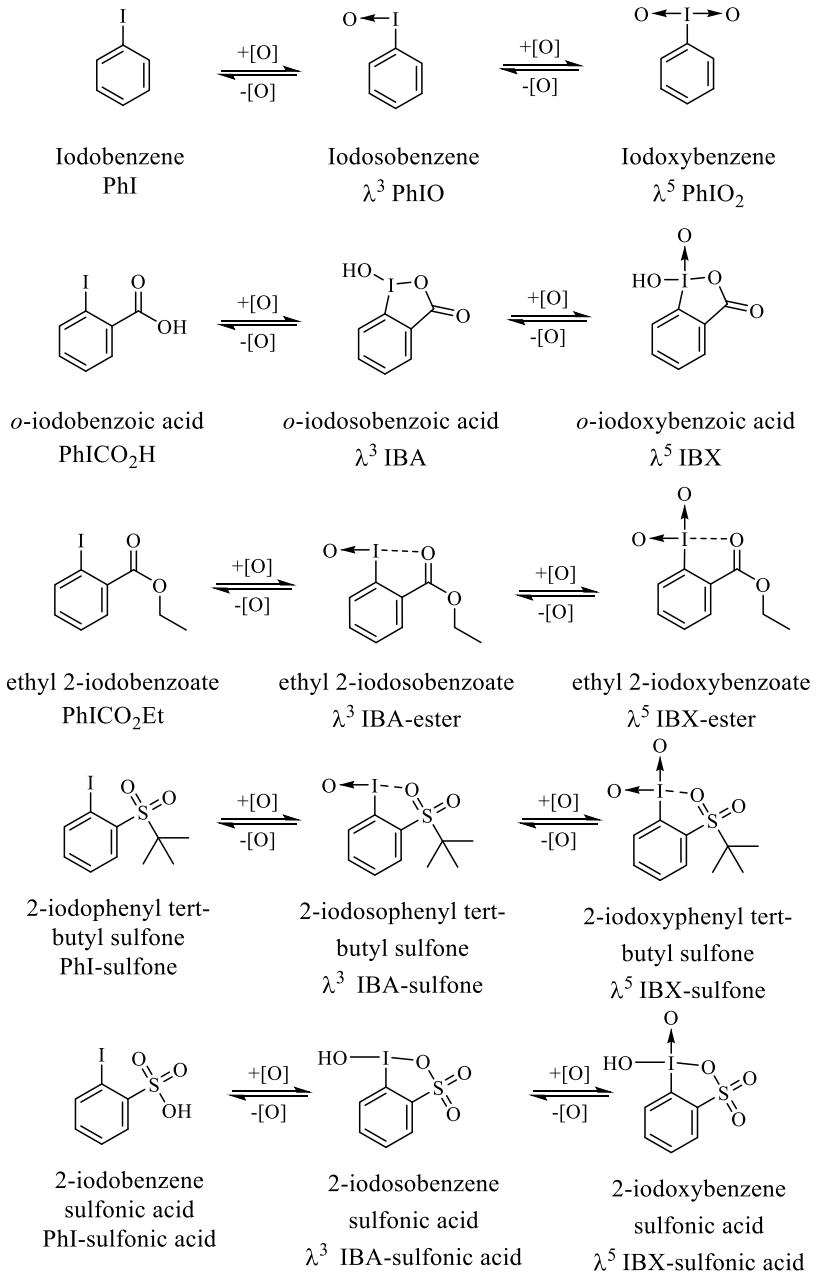

cleavage at tryptophan residues,[13,14] and also serves as a precursor to other hypervalent group-transfer reagents. Those known group-transfer reagents include (i) ethynylbenziodoxol-(on)e that can be used in alkynylations;[15] (ii) 1-trifluoromethyl-1,2-benziodoxol-3(1*H*)-on, commonly referred to as Togni's reagent that can perform transfer of a trifluoromethyl group;[16] and (iii) azidobenziodoxolone, a relatively stable azide source.[17] In short, hypervalent iodine reagents are versatile, O-atom, and other group-transfer reagents.

Although nominally described as hypervalent and often drawn with an I═O double bond, the I → O bond is more accurately described as a dative bond.[18] For simplicity, in this work, the O-atom transfer reagents will be referred to using the hypervalent nomenclature. A summary of abbreviations used in the following is presented in Scheme 1 along with closer-to-true representations of their bonding as discussed further elsewhere.[18]

A primary hypothesis examined in the present work is that chemically versatile O-atom and group-transfer reagents based on Ar−I such as iodosobenzoic acid (IBA) or iodoxybenzoic acid (IBX) and their derivatives can be synthesized electrochemically using water as the O-atom source for potential use in O-atom transfer catalysis. There is little reported in terms of electrocatalysis or electrosynthesis of O-atom transfer reagents, except for a report of the electrochemical formation of iodoxybenzoic acid (IBX) from iodobenzoic acid precursor ($PhICO_2H$) in aqueous solutions.[19,20] This stands in contrast to the extensive progress with the electrochemistry of hypervalent iodine as mediators in electrocatalytic reactions such as fluorination and other group-transfer reactions.[21−26]

The aforementioned PhIO, IBA, and IBX reagents have been extensively explored, but their use is limited by their relatively low solubility due to strong intermolecular bonding at the highly polar iodine center.[9,10] Reagents such as 2-iodoxyphenyl

https://doi.org/10.1021/acssuschemeng.1c01315
ACS Sustainable Chem. Eng. 2021, 9, 10453−10467

Scheme 2. Chemical Synthesis of (a) IBA Using Periodate, Persulfate, and O_2 as Oxidants,[29] (b) IBA-Sulfone Using Peracetic Acid or Chlorine Followed by Hydrolysis,[31] and (c) IBX-Sulfone (or IBX-Sulfonic Acid) Using Oxone[27]

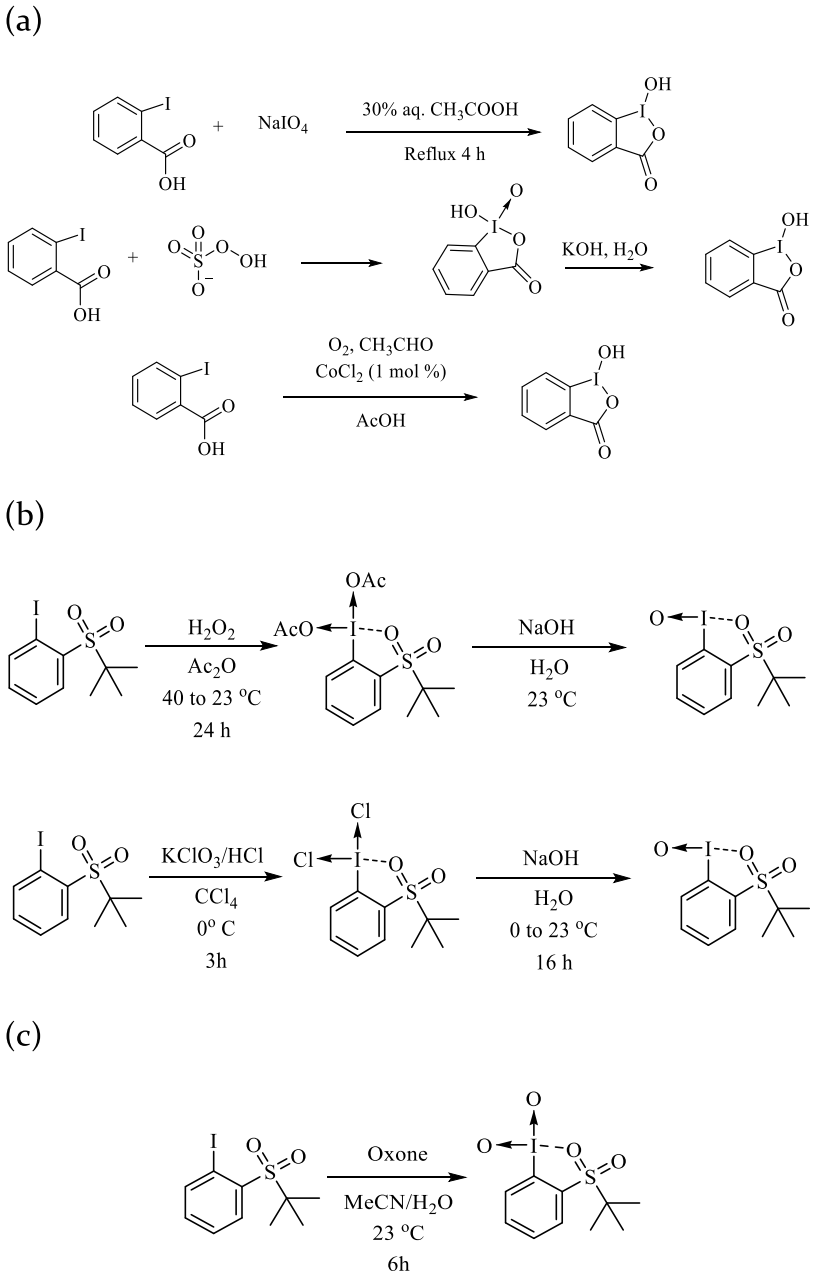

tert-butyl sulfone (IBX-sulfone) and 2-iodoxybenzene sulfonic acid (IBX-sulfonic acid) are similar in reactivity and utility to PhIO and IBX, but are significantly more soluble and often more reactive. For example, IBX-sulfonic acid has been reported to oxidize most organic solvents including methanol and acetonitrile on contact.[27] Additionally, IBX-sulfonic acid has also been used catalytically for chemically driven alcohol oxidation in near-quantitative yields using oxone as the terminal, stoichiometric oxidant.[11,28]

Although IBA is relatively simple to synthesize and isolate via chemical oxidation of *o*-iodobenzoic acid ($PhICO_2H$) using IO_4^- and acetic acid,[29] or through hydrolysis of IBX (Scheme 2), synthetic routes are limited by the use of stoichiometric oxidants.[30,31] Recent work used O_2 as a green chemistry oxidant to synthesize IBA and other λ^3-hypervalent iodine species which were then used with other oxidation and oxygenation reactions.[32−34] Other λ^3-iodine species are often difficult to obtain due to their reactivity and propensity toward disproportionation to the ArI and λ^5-species,[35] while the synthesis of λ^5-reagents typically requires the use of a powerful oxidant such as oxone (Scheme 2).[11,25,28]

Herein, we report the selective electrochemical synthesis of hypervalent iodine reagents iodosobenzoic acid (IBA), ethyl-2-iodosobenzoate (IBA-ester), 2-iodoxyphenyl *tert*-butyl sulfone (IBX-sulfone), and a reactive mixture of 2-iodosobenzene sulfonic acid (IBA-sulfonic acid) and 2-iodoxybenzene sulfonic acid (IBX-sulfonic acid) (Scheme 3). Isolated materials were obtained where possible and the products were characterized using ^1H, ^{13}C NMR, Fourier transform infrared (FT-IR) spectroscopy, and mass spectrometry confirming the formation of IBA, IBA-ester, IBX-sulfone, and IBA/IBX-sulfonic acid. We also conduct initial mechanistic studies in the form of ^{18}O

https://doi.org/10.1021/acssuschemeng.1c01315
ACS Sustainable Chem. Eng. 2021, 9, 10453−10467

Scheme 3. Electrochemical Synthesis of Hypervalent Iodine Reagents via Bulk Electrolysis at a Glassy Carbon Electrode with H_2O as the O-Atom Source

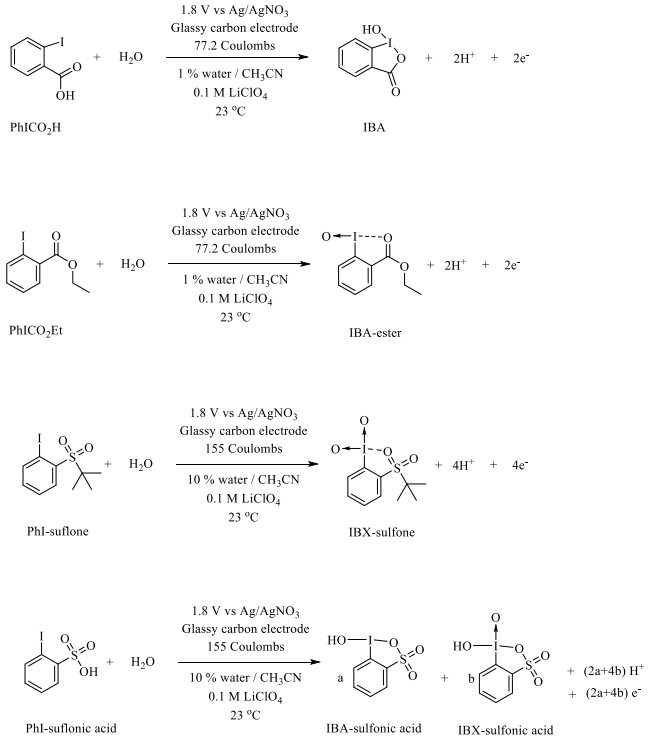

labeling studies using $H_2{}^{18}O$ revealing that the majority of the at least initial O-atoms present in the oxygenated, hypervalent iodine product comes from surface oxide species on the (oxidized) glassy carbon. This carbon-surface oxide is regenerated using $H_2{}^{18}O$ from solution leading to ^{18}O incorporation into the product, thereby using H_2O as an O-atom source. The implications for other hypervalent iodine group-transfer reagents are discussed as are implications for electrochemical and photoelectrochemical oxygenations using water as the O-atom source.

EXPERIMENTAL SECTION

General Considerations. All chemicals were purchased of the highest possible purity and used without further purification. $PhICO_2H$, $PhICO_2Et$, and PhI-sulfonic acid were purchased from chemical suppliers, whereas PhI-sulfone was synthesized according to literature methods as described in the Supporting Information.[34] Solutions were prepared in glassware dried in an oven overnight at 200 °C and the $LiClO_4$ was dried by heating at 200 °C for 2 days. MeCN was obtained from a solvent still and the MeCN $LiClO_4$ solutions were degassed for >30 min using N_2 bubbled through MeCN (to prevent evaporation of the MeCN) once the solution was added to the U-cell. Glassy carbon electrodes were cut from a 2-mm-thick sheet using a diamond-tipped saw. Except when noted, the electrodes were cleaned between experiments by sonicating in aqueous ascorbic acid (to help remove insoluble/oxidizing material) and then polishing using 0.05 μm alumina slurry followed by sonicating in water for 5 min and then sonicating in ethanol for 5 min. All potentials are referenced against an $Ag/AgNO_3$ CH_3CN solution containing 0.01 M $AgNO_3$ and 0.1 M $LiClO_4$. All ^1H NMR experiments were conducted either by adding CD_3CN to reaction solutions or by dissolving the product in CD_3CN. However, IBA is only soluble in dimethylsulfoxide (DMSO), and in that case, d_6-DMSO was added to electrolysis solutions or the product was dissolved in d_6-DMSO for NMR. For the quantitative ^1H NMR, the internal standard dimethyl sulfone ($DMSO_2$) was used because it is not easily oxidizable and commonly used in quantitative NMR (qNMR).[36]

Electrochemical experiments were conducted using a Gamry 600+ potentiostat or a Bio-Logic VSP-300. NMR spectra were collected on a 400 MHz Bruker spectrometer. FT-IR spectra were collected on a Bruker Tensor II in attenuated total reflectance (ATR) mode. Mass spectrometry was collected on a Thermo Finnigan LTQ electrospray ionization mass spectrometer (ESI-MS).

Safety Considerations. Many hypervalent iodine species are known to explosively decompose at high temperatures and there are accounts of explosions while drying IBX.[37] These initial reports of explosions are likely caused by side products formed during the synthesis since analytically pure samples of IBX are not shock-sensitive and but do explode at elevated temperatures.[37,38] Hence, syntheses and reactions were carried out on small 20 mL scales to mitigate the associated risk (except when the scale-up electrolyses of $PhICO_2H$ were conducted). The reported isolated yields are, as a consequence, unoptimized lower limits meaning that the isolated yield can be improved by prolonging electrolysis beyond 100% theoretical conversion and on a larger scale where collection of the product will be more efficient. Furthermore, because unknown, potentially explosive,[37,38] side products can be formed (i.e., when the Faradaic efficiency to the characterized product is <100%), all reactions were quenched by slowly adding a reductant of solid ascorbic acid (standard potential of ≈+0.35 V vs normal hydrogen electrode (NHE))[39] to the reaction solutions in the presence of KI/starch (which is blue in the presence of oxidant and turns colorless upon quenching) before disposing in the appropriate waste stream.

Electrochemistry of the Iodine Precursors. Cyclic voltammograms were collected using a 0.07 cm^2 glassy carbon disk electrode in a vial containing 20 mM $PhICO_2H$, $PhICO_2Et$, PhI-sulfone, or PhI-sulfonic acid with 0.1 M $LiClO_4$ supporting electrolyte, in degassed CH_3CN with no added water or water added at 1 or 10 v/v%. The amount of water present in the $MeCN/LiClO_4$ solution was determined to be 180 ppm via Karl Fischer titration. The $Ag/AgNO_3$ reference electrode and carbon felt counter electrode were placed as close as possible to the working electrode ≤1 cm.

Electrochemical Synthesis and Characterization of Hypervalent Iodine Reagents. Bulk electrolyses were carried out in a U-cell (20 mL working solution unless otherwise stated) with the reference and large working electrode (~8 cm^2 glassy carbon) on the same side and separated from the counter electrode on the other side of the U-cell by a fine glass frit with a 5−8 cm separation of the working and counter electrodes while ≤1 cm separation of the working and reference electrodes (Figure S1). Chronocoulometry was conducted at 1.8 V with vigorous stirring, and 250 μL aliquots were occasionally taken for ^1H NMR. We sometimes had issues with our potentiostat at early time points in experiments with an overload of the control amplifier. These overloads indicate that a sufficient potential cannot be applied at the counter electrode to meet the current demand and are caused by the (relatively) high currents being passed by the potentiostat when using the larger glassy carbon electrode, the relatively insulating nature of the organic solvent, or because we did not use a sacrificial reductant at the counter electrode (thereby avoiding crossover effects between electrode cell compartments). To mitigate against this, we used a carbon felt counter electrode (to maximize counter electrode surface area) and adjusted the potentiostat compliance to allow for a larger (more negative) voltage to be applied at the counter electrode.

In the case of $PhICO_2H$ electrolysis in the presence of 1% added water a white precipitate was observed and collected via vacuum filtration through a fine fritted filter followed by 3 × 50 mL washes with acetonitrile to remove unreacted $PhICO_2H$ and $LiClO_4$, then dried on the filter overnight. The product was collected and weighed in a vial. ^1H, ^{13}C NMR, and FT-IR spectra were collected on the product.

To test the scalability of this method bulk electrolysis was conducted with 1% added water and 100 mM $LiClO_4$ on three different scales: (i) the aforementioned 20 mL, 20 mM $PhICO_2H$

https://doi.org/10.1021/acssuschemeng.1c01315
ACS Sustainable Chem. Eng. 2021, 9, 10453−10467

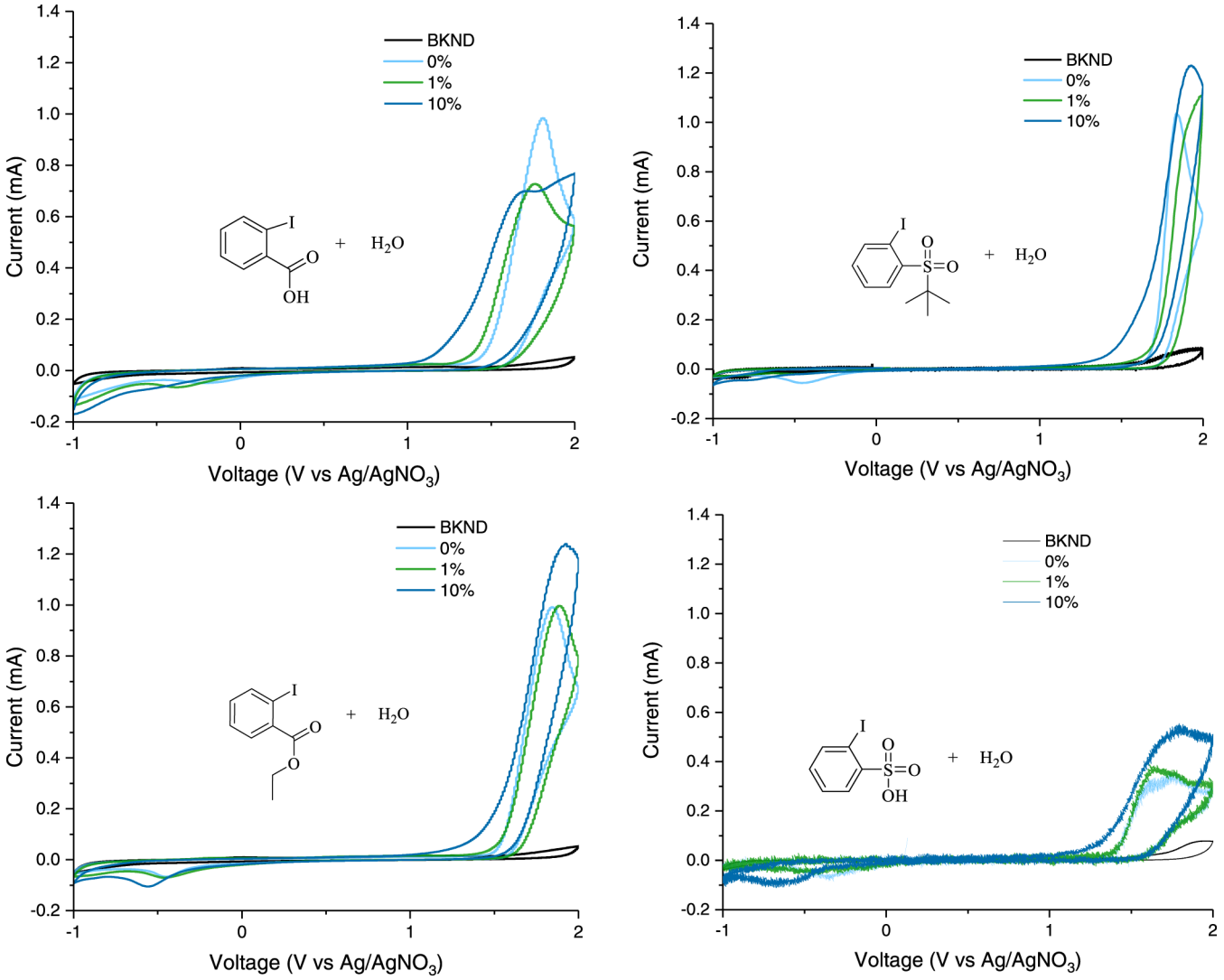

Figure 1. Cyclic voltammograms of $PhICO_2H$ (top left), $PhICO_2Et$ (bottom left), PhI-sulfone (top right), and PhI-sulfonic acid (bottom right), with no added water (cyan), 1% (green), and 10% (blue) added water (v/v). All CVs were acquired with 0.1 M $LiClO_4$ supporting electrolyte, 20 mM $PhICO_2H$ (or $PhICO_2Et$), CH_3CN solvent, 0.07 cm^2 glassy carbon working electrode, and $Ag/AgNO_3$ reference electrode with scans beginning in the positive direction at 100 mV/s. In each case, increasing water increases the anodic current, indicating water's involvement in the net oxidation reaction. Background, control CVs of the dry, 1%, and 10% added water (but no PhI-based substrate present) are shown in Figure S3 in the Supporting Information and reveal little change, especially compared to the current observed from the addition of the PhI-derivatives.

(99.2 mg) at 100% conversion; (ii) a 40 mL, 20 mM $PhICO_2H$ (198 mg) solution electrolyzed to 85% conversion; and (iii) a 250 mL, 20 mM $PhICO_2H$ (1.24 g) solution electrolyzed for 48 h to 94% conversion. In each case, the resulting precipitate was collected and its identity was confirmed using ^1H and ^{13}C NMR and FT-IR. Quantitative NMR (qNMR) using the method of standard addition was conducted on the filtrate solution obtained from the 250 mL scale bulk electrolysis. To do so, four NMR tubes were prepared containing 0.5 mL total solution volume that consisted of 0.25 mL of the filtrate solution; 0.25 mL of d_6-DMSO; and 20 mM dimethyl sulfone ($DMSO_2$) as a reliable, chemically inert, internal standard;[36] and authentic IBA spiked to final concentrations of 0, 5, 10, and 20 mM. The four ^1H NMR peaks in the aromatic region of IBA were individually integrated and divided by the integration of the dimethylsulfoxide internal standard. The normalized intensity of each peak was plotted against the concentration of added IBA and the concentration of IBA in the original solution was determined by averaging the absolute value of the x-intercept of the linear fits and doubling to account for the dilution when mixing the ^1H NMR solutions.

For the case of electrolysis of $PhICO_2Et$ in the presence of 1% water, the product is soluble in acetonitrile meaning that it cannot be collected via filtration. Instead, the reaction solution was placed into a vial and the $LiClO_4$ was precipitated using a 1:1 molar equivalent of KF with vigorous stirring for 1 h at room temperature. The vial was then placed into an ice bath for 45 min to allow for the precipitation of $KClO_4$ and LiF. Next, the precipitated salts were removed via filtration through a fine fritted filter. The resulting solution was rotary evaporated to obtain a yellow oil. The collected product was characterized via ^1H and ^{13}C NMR in addition to FT-IT in ATR mode and electrospray ionization (ESI) mass spectrometry in acetonitrile in positive-ion mode.

The total amount of IBA-ester was determined from these collections using the integrated peak intensity in ^1H NMR (these calculations are presented in the Supporting Information for the interested reader).

Isolation of the product from the bulk electrolysis using PhI-sulfone and PhI-sulfonic acid in the presence of 1 or 10% water proved difficult. The product remained soluble in solution and addition of KF to reaction solutions (to precipitate the electrolyte) caused significant changes in the ^1H NMR spectrum indicating structural changes.

https://doi.org/10.1021/acssuschemeng.1c01315
ACS Sustainable Chem. Eng. 2021, 9, 10453−10467

Hence, the product analysis was limited to ^{1}H NMR. The Faradaic efficiency of the reactions was determined using the relative peak intensity of the most upfield (and unobscured) ^{1}H NMR peak in the aromatic region of the starting material compared with the most unobscured peak for the generated hypervalent iodine species.

Electrochemical Synthesis of Hypervalent Iodine Using $H_2{}^{18}O$. Bulk electrolysis was conducted in a U-cell (20 mL working volume) reaction vessels using 1% added water that consisted of ^{18}O-labeled water (97 atom %) in the working compartment with 0.1 M $LiClO_4$ and 20 mM $PhICO_2Et$. Taking into account the amount already present in MeCN/$LiClO_4$ (180 ppm), the amounts of ^{18}O and ^{16}O are 95 and 5 atom %, respectively. The solutions containing the added $^{18}OH_2$, electrolyte, and substrates were mixed and placed into glassware that had been dried at 230 °C overnight prior to addition of the electrodes and electrolysis. Electrolysis was conducted until 2e$^-$/$PhICO_2Et$ had accumulated. The products were collected in the same manner as mentioned previously for $PhICO_2Et$. Electrospray ionization mass spectrometry (ESI-MS) was conducted on the ^{18}O-labeled product from the electrolysis of $PhICO_2Et$. Isotopic labeling experiments were not conducted with PhI-sulfone or PhI-sulfonic acid due to their reactivity and difficulty in isolation.

Consecutive $H_2{}^{18}O$ Electrolyses Using the Same Electrode. Bulk electrolysis was conducted using $PhICO_2Et$ in the same manner as above except instead of cleaning the electrode between experiments the electrode was immediately moved into a fresh electrolyte solution containing unreacted $PhICO_2Et$. Bulk electrolysis was then again conducted on the $PhICO_2Et$ solution until complete electrolysis had occurred. This process was repeated twice for a total of three electrolysis solutions. The $PhICO_2Et$ from each electrolysis was then collected using the KF precipitation method and analyzed via ESI-MS.

RESULTS AND DISCUSSION

Cyclic Voltammetry of Iodine Species in CH_3CN with and without Added Water. The cyclic voltammograms of $PhICO_2H$, $PhICO_2Et$, PhI-sulfone, and PhI-sulfonic acid (20 mM) in acetonitrile containing 0.1 M $LiClO_4$ supporting electrolyte are shown in Figure 1 with no added water and with 1 or 10 v/v% added water (the native water in the MeCN/$LiClO_4$ was determined to be 180 ppm (i.e., ∼0.018% v/v%) by Karl Fischer titration). The characteristics of the oxidative wave in all cases are affected by the presence of water. In the case of $PhICO_2H$ the onset of oxidation is shifted to a lower potential, the peak current is diminished and the peak appears to separate into two distinct electron-transfer events at 10% water (Figures 1 and S2 of the SI). For the case of $PhICO_2Et$ the peak current actually increases with added water and the formation of a species which is reduced upon scanning to −0.5 V is observed. A similar trend is observed with PhI-sulfone and PhI-sulfonic acid where the peak potential and peak current are shifted to higher voltage and higher current with greater water content (note that the solutions for PhI-sulfonic acid remained slightly turbid, indicating incomplete dissolution of PhI-sulfonic acid which likely accounts for the amount of noise observed in the CV, Figure 1). Controls with 0, 1, and 10% added water in the absence of ArI precursors are presented in Figure S3 in the Supporting Information and demonstrate virtually no change in the anodic current.

We initially interpreted these observations to be consistent with electrochemical oxidation of the ArI precursors which subsequently reacts in a chemical step involving water (an EEC mechanism, vide infra). However, the anodic current is not linear with respect to the water concentration as one might expect if it were involved with a fast, chemical step. Nonetheless, we decided to pursue our hypothesis of the electrochemical oxidation involving water to form hypervalent species as shown in Scheme 1. Hence, next we conducted bulk electrolysis to accumulate enough material for further analysis and characterization.

Bulk Electrolysis of $PhICO_2H$ in the Presence of Water and Characterization of the Isolated Material. Bulk electrolysis was conducted at 1.8 V vs $Ag/AgNO_3$ on 20 mL solution of a 20 mM $PhICO_2H$ (0.4 mmol, substrate) solution in the working side of a U-cell with a large ∼8 cm^2 glassy carbon electrode (Figure 2; see Figures S1 and S4 in the Supporting Information for pictures of the U-cell). For solutions of this size and concentration and assuming 2e$^-$/mol, a 100% theoretical conversion of 0.4 mmol of $PhICO_2H$ corresponds to 77.2 C of charge passed through the electrode (calculations are provided in the Supporting Information for the interested reader). The reaction progress was monitored via ^{1}H NMR and compared with authentic IBA and IBX (Figures 3 and S5 in the Supporting Information). ^{1}H, ^{13}C NMR, and FT-IR of this product confirmed the identity of the collected precipitate to be λ^3-IBA and not λ^5-IBX (Figures 3a, S5, S6 and S7 in the Supporting Information).

The $PhICO_2H$ and IBA relative concentrations were calculated using the relative peak intensities of their respective ^{1}H NMR peaks. The Faradaic efficiency remains near 100% for the first half of the reaction without the appearance of any other detectable byproducts (Figure 3b). The Supporting Information provides an explanation of the calculations to determine the Faradaic efficiency. At approximately 50% conversion of $PhICO_2H$ oxidation, a white precipitate appears (Figure S4 in the Supporting Information). After full theoretical (100%) conversion (77 C), the white precipitate was collected via filtration and weighed 30 mg, 28% isolated yield at this scale (yields in the same U-cell configuration were reproducible). ^{1}H NMR of the filtrate solution reveals that residual IBA product remains soluble in MeCN along with a small amount of unreacted starting material. Importantly, no other peaks were observed in the ^{1}H NMR, so contributions from the decomposition of the hypervalent iodine precursor or product are minimal.

Conducting the bulk electrolysis at a 40 mL scale to 85% conversion produced 105 mg of material (180 mg theoretical, a 58% isolated yield). Bulk electrolysis of a 250 mL, 20 mM

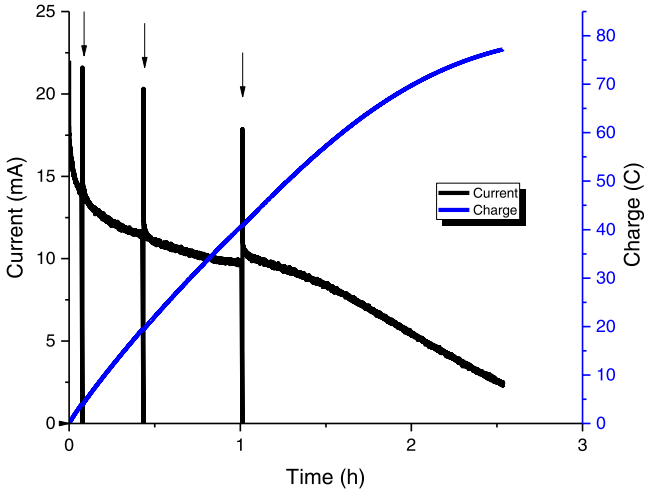

Figure 2. Example bulk electrolysis of $PhICO_2H$ with 1% water current shown in black and total accumulated charge shown in blue. Black arrows indicate the current spikes where the electrolysis was paused to take aliquots for ^{1}H NMR.

https://doi.org/10.1021/acssuschemeng.1c01315
ACS Sustainable Chem. Eng. 2021, 9, 10453−10467

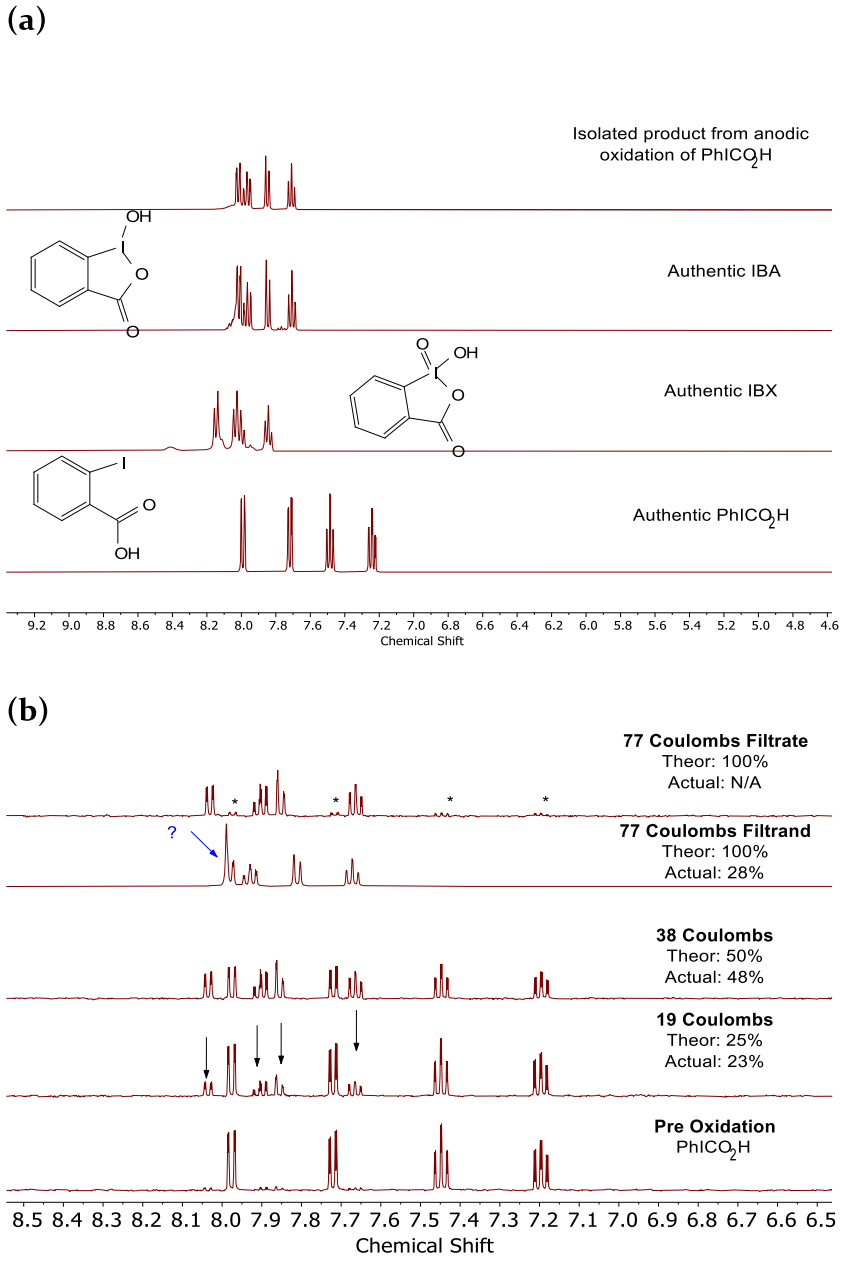

Figure 3. (a) Comparison of the ^{1}H NMR aromatic region of $PhICO_2H$, IBX, IBA, and the isolated material from the bulk oxidation in d_6-DMSO added and (b) ^{1}H NMR aromatic region from bottom to top of $PhICO_2H$ before oxidation, at 19 and 38 C of charge passed, the precipitate isolated after 77 C of oxidation (filtrand) and the filtrate from the same solution. Black arrows indicate the peaks consistent with IBA product, and the asterisks indicate the peaks of the $PhICO_2H$ starting material. Detection of IBA in the filtrate demonstrates that a small amount remains soluble and was not collected by filtration. The appearance of a singlet at ca 8.0 ppm due to an unknown species sometimes occurs when isolating IBA from the electrolysis solution. However, the ^{1}H NMR spectrum of bulk electrolysis is well matched to the IBA spectrum demonstrating the formation of IBA and not λ^5-IBX as the main product. The ^{13}C NMR and FT-IR spectra also support IBA as the primary product (Figures S6 and S7 in the Supporting Information).

$PhICO_2H$ solution (5 mmol) electrolyzed 48 h to 900 C (94% theoretical conversion, 1.24 g theoretical yield), produced 597 mg of isolated product (a total isolated yield of 48%). Quantitative ^{1}H NMR (qNMR) of the electrolysis filtrate solution using $DMSO_2$ as an internal standard showed 7.6 ± 0.2 mM IBA, corresponding to 502 ± 14 mg IBA remaining in solution (Figure S8 in the Supporting Information).[36] Hence, the total amount of IBA is ∼1100 mg (corresponding to an 89% Faradaic efficiency). The remainder of the unaccounted material can be attributed to unreacted $PhICO_2H$ or IBA that has crossed the glass frit into the other side of the U-cell during the electrolysis. These results indicate both that scale-up is possible, but that an optimized scale-up will require its own, separate study, which is not surprising given the known issues of scale-up in general[40] and electrochemical scale-up in particular.[41]

Bulk Electrolysis of $PhICO_2Et$ in the Presence of Water and Characterization of the Isolated Material. Bulk electrolysis was conducted using $PhICO_2Et$ in the same conditions as above (20 mL working solution, 1% water, 20 mM $PhICO_2Et$, 1.8 V). Again, the reaction progress was monitored throughout the reaction and was compared with

https://doi.org/10.1021/acssuschemeng.1c01315
ACS Sustainable Chem. Eng. 2021, 9, 10453−10467

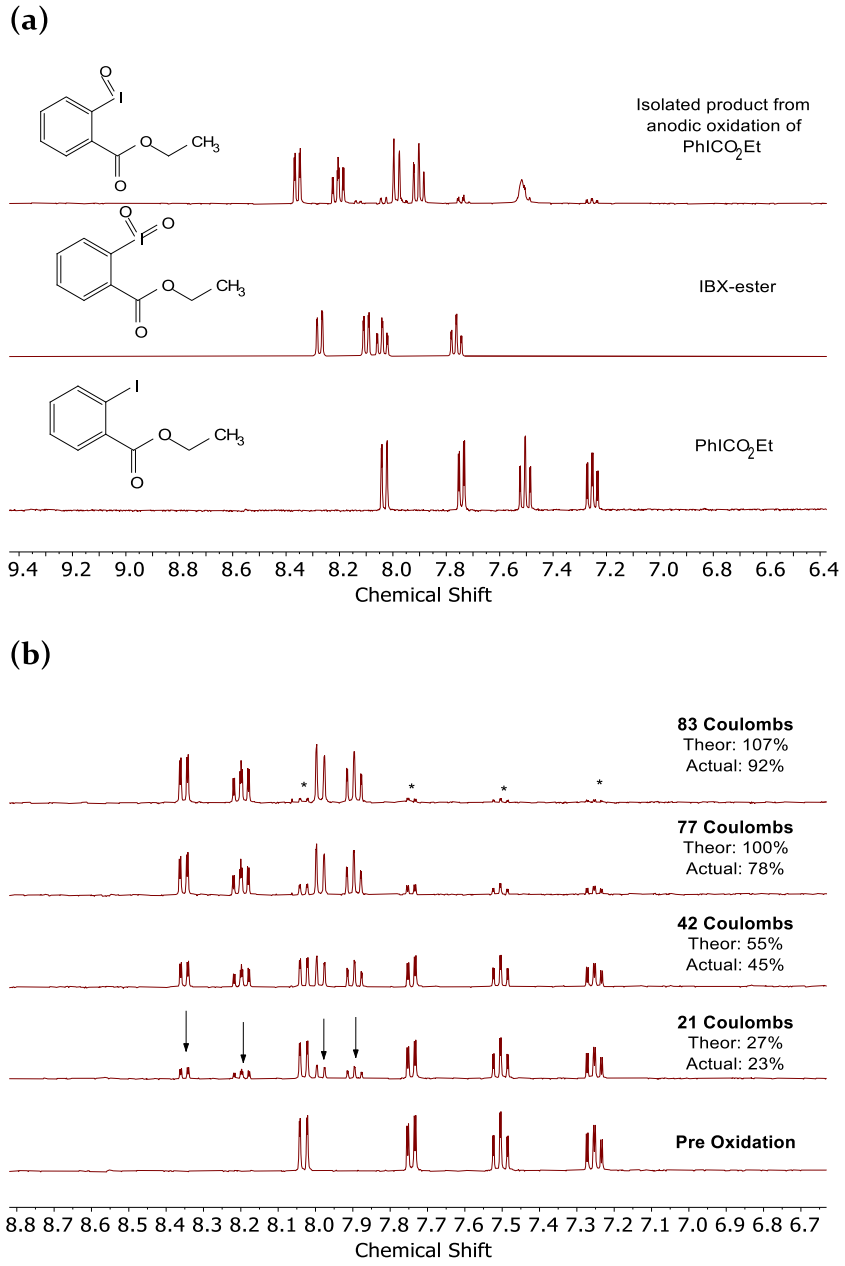

Figure 4. (a) ^{1}H NMR aromatic region from bottom to top of $PhICO_2Et$, IBX-ester, and the isolated material after 77 C of electrolysis ($2e^{-}$/$PhICO_2Et$) with d_3-MeCN. ^{1}H NMR spectrum of the isolated material does not match either IBX-ester or $PhICO_2Et$. (b) ^{1}H NMR aromatic region of the $PhICO_2Et$ solution from bottom to top before oxidation, 21, 42, 77, and 83 C of charge passed. The peaks labeled with asterisks (*) in the top spectrum correspond to the unconverted $PhICO_2Et$ following the expected triplet, triplet, doublet, doublet as is typically the case for $PhICO_2H$ derivatives (see also Figure 3). The peaks in the spectrum labeled with arrows correspond to the formation of the new product.

authentic IB**X**-ester (Figures 4 and S9 in the Supporting Information). We could not compare the electrolyzed material with authentic IB**A**-ester because it has not been previously synthesized, to our knowledge. IBA-ester cannot be synthesized using traditional methods because the ester hydrolyzes during the traditional chemical syntheses shown back in Scheme 2. Notwithstanding, the following evidence is consistent with and supportive of the product being IB**A**-ester: (i) the mass spectrum of the isolated material from the electrolysis of $PhICO_2Et$ has a primary peak that is consistent with the molar mass for the protonated HIBA-ester^{+} (~293 g/mol, Figure S11 in the Supporting Information) and, again, not the λ^5-IBX-ester (expected at ~309 g/mol). Additionally, (ii) comparison of the ^{1}H NMR of the electrolyzed solution with IBX-ester exhibits peaks inconsistent with the formation of IBX-ester (Figures 4 and S9 in the Supporting Information), specifically the aromatic protons of the IBX-ester electrolysis follow triplet, triplet, doublet, doublet from upfield to downfield in the starting material, but the observed λ^3-product protons are shifted upfield and switched to triplet, doublet, triplet, doublet, indicating a similar resonance pattern with the oxidized iodine atom as was observed with the free acid, IBA; (iii) the ^{13}C NMR does not show a peak near 150 ppm which is expected for λ^5 species (Figure S10 in the Supporting Information)[42] and (iv) FT-IR of the electrolyzed $PhICO_2Et$ (Figures S12 and S13 in the Supporting Information) is similar to that of the free acid IBA in that the C═O stretch peak appears at 1613 cm^{-1}, which has been attributed to the C═O

https://doi.org/10.1021/acssuschemeng.1c01315
ACS Sustainable Chem. Eng. 2021, 9, 10453−10467

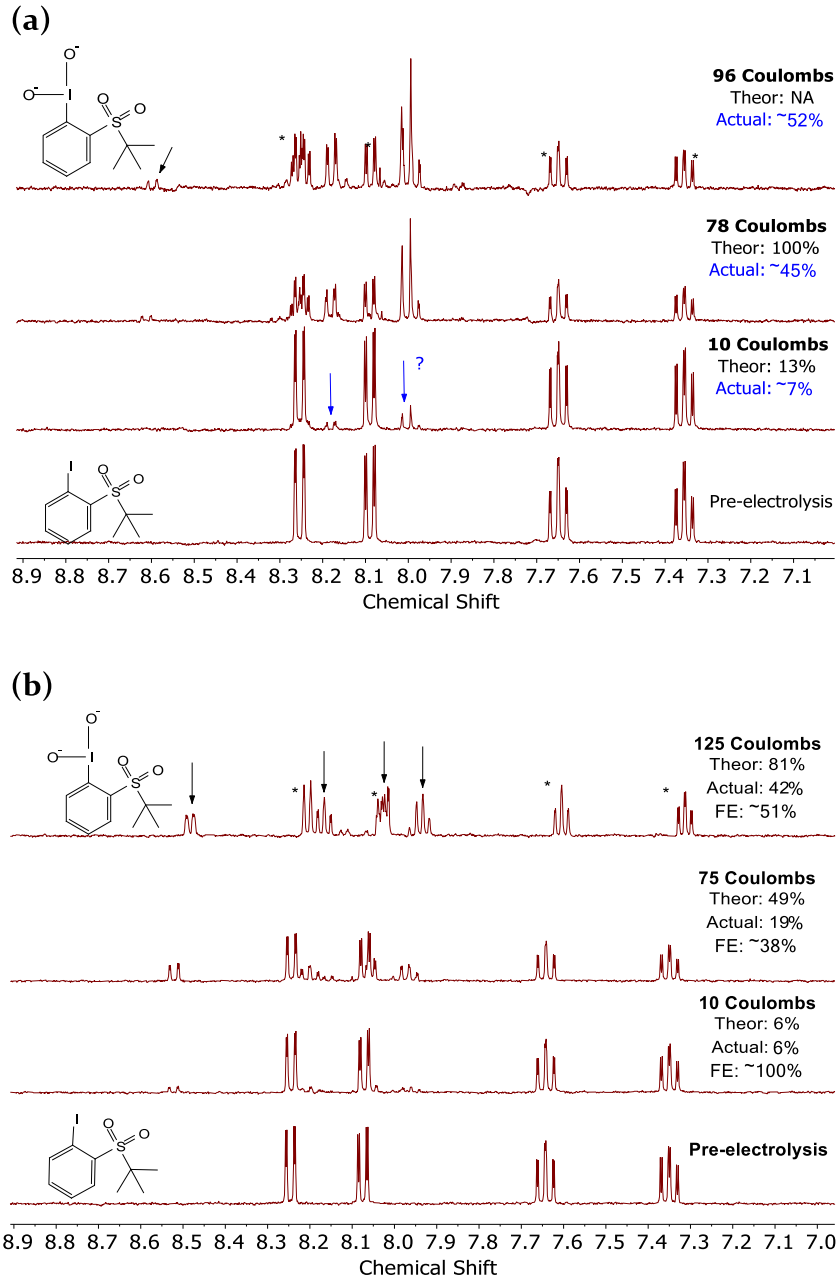

Figure 5. ^{1}H NMR aromatic region of 20 mM PhI-sulfone, 100 mM $LiClO_4$ supporting electrolyte with (a) 1% and (b) 10% added water (v/v%) showing the peaks before electrolysis; for samples taken during electrolysis, the charge accumulation is shown on the right-hand side. The theoretical yield for the unknown species in (a) was calculated assuming $2e^-$/molecule and for (b) IBX-sulfone based on $4e^-$/molecule. The ^{1}H NMR peaks for IBX-sulfone match the literature.[34]

involved with the pseudocyclic species (Figure S13 in the Supporting Information).[43] Hence, anodic oxidation of PhI-esters provides a synthetic route to the novel hypervalent iodine reagent λ^3-IBA-ester shown in Scheme 1, and by implication other hypervalent iodine esters as well.

Interestingly, electrolysis of $PhICO_2Et$ did not yield a precipitate, likely because the intermolecular bonding that forms the polymeric precipitate is interrupted by the ethyl ester.[30] However, using integration of the ^{1}H NMR peaks, the Faradaic efficiency of the electrolyzed $PhICO_2Et$ is ~78% for the production of IBA-ester (Figure 4b). No other peaks are observed in the aromatic region, indicating substrate-to-product selectivity for the production of IBA-ester.

Bulk Electrolysis of PhI-Sulfone in the Presence of Water and Characterization of the Produced Material. Electrolysis of PhI-sulfone (20 mM) was conducted at 1.8 V on a 20 mL solution and the reaction progress was monitored using ^{1}H NMR. A variety of products was observed when conducting the oxidation in 1% water (Figures 5a and S14 in the Supporting Information), including a hitherto unidentified initial product (which does not match the expected ^{1}H NMR resonances of IBA-sulfone) and eventually IBX-sulfone. When the oxidation of PhI-sulfone is conducted in 10% water, only IBX-sulfone is observed and is produced at ~51% Faradaic efficiency (Figure 5b), estimated from the ^{1}H NMR integration. Attempts to isolate the products from bulk electrolysis using KF to precipitate the $LiClO_4$ proved

https://doi.org/10.1021/acssuschemeng.1c01315
ACS Sustainable Chem. Eng. 2021, 9, 10453−10467

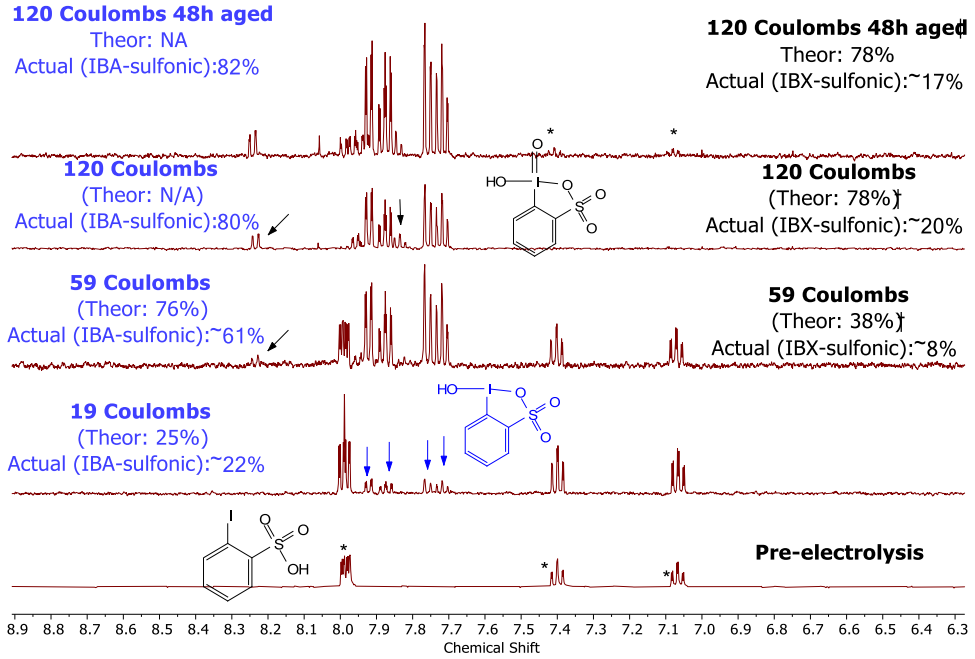

Figure 6. ^{1}H NMR aromatic region of 20 mM PhI-sulfonic acid, 100 mM $LiClO_4$ supporting electrolyte with 10% added water (v/v%) showing peaks before electrolysis and after 19, 59, and 120 C of charge passed and the same 120 C solution aged 2 days. ^{1}H NMR peaks for IBA- and IBX-sulfonic acid match the literature.[27,28,44] †The theoretical yield for IBX-sulfonic acid was determined assuming full conversion to IBX-sulfonic acid (i.e., 4e$^-$/molecule). See the Supporting Information for a sample calculation of the Faradaic efficiency and additional discussion.

unsuccessful in that significant changes in the ^{1}H NMR are observed before and after addition of KF—potentially indicating substitution of the [O] with F$^-$.

Bulk Electrolysis of PhI-Sulfonic Acid in the Presence of Water and Characterization of the Produced Material. Because PhI-sulfonic acid does not dissolve fully in just 1% water in MeCN at room temperature, the bulk anodic oxidation electrolysis of PhI-sulfonic acid was conducted under 10% water under MeCN conditions. Specifically, bulk electrolysis on a 20 mL solution of PhI-sulfonic acid (20 mM. 0.4 mmol) was conducted. The theoretical amount of charge for complete, 100% conversion of PhI-sulfonic acid into IBA-sulfonic acid and IBX-sulfonic acid is 77 and 154 C, respectively (i.e., 2e$^-$/molecule and 4e$^-$/molecule, respectively). The bulk electrolysis led first to the formation of IB**A**-sulfonic acid until >60 C of charge had accumulated, after which further oxygenation to IB**X**-sulfonic acid became observable by ^{1}H NMR (Figures 6 and S15 in the Supporting Information). After 120 C of charge had accumulated all of the starting material was consumed and ∼20% of the IBA-sulfonic acid was converted to IBX-sulfonic acid. Hence, after a significant amount of IBA-sulfonic acid accumulates it can be anodically oxidized again to form the more reactive IBX-sulfonic acid (Figure 6). By totaling the amount of charge associated with both IBA-sulfonic acid and IBX-sulfonic acid, the total Faradaic efficiency was determined to be 78% post 120 C of electrolysis, respectively (see the Supporting Information for additional details). Interestingly, after aging the electrolyzed solution for 2 days, the ^{1}H NMR peak intensity of IBX-sulfonic acid is decreased and a slight recovery of IBA- and PhI-sulfonic acid is observed, consistent with previous reports that IBX-sulfonic acid is reactive toward oxidation of common organic molecules, even relatively inert ones such as acetonitrile.[27,28] Hence, the Faradaic efficiency is ≥78% given the highly reactive nature of the IBX-sulfonic acid—a desirable feature for subsequent O-atom transfer catalysis.

In short, $PhICO_2H$, $PhICO_2Et$, PhI-sulfone, and PhI-sulfonic acid can be electrochemically oxidized to form hypervalent products with isolated yields ranging from 28 to 48% and Faradaic efficiency ranging from 51 to 89% (Table S1 in the Supporting Information). A comparison of the chemical synthesis procedures to the electrochemical synthesis procedures developed herein is presented in the Supporting Information.

Electrochemical Mechanism of ArI → O Formation. A better understanding of the underlying electrochemical mechanism is needed before attempts to scale up and optimize both the synthesis and use of hypervalent iodine reagents. Hence, we started by considering three prospective, arguably most likely mechanisms (Scheme 4):[45] (i) an EEC mechanism wherein the ArI undergoes a 2e$^-$ oxidation at the electrode (i.e., double-oxidized) and then diffuses away from the electrode, where it is quenched by nucleophilic attack by water; (ii) an ECE mechanism where ArI is oxidized by 1e$^-$ to form an intramolecularly stabilized radical intermediate which reacts with water and then undergoes a subsequent 1e$^-$ oxidation to form the product; and finally previously little considered (iii) an EEC-electrode mechanism wherein an O-atom from one or more of several possible glassy carbon O-containing sites[46] (Scheme 4, mechanism (iii)) is transferred directly to form the hypervalent iodine product.

We had initially hypothesized that the EEC mechanism was the most likely path given that addition of water had an effect on the anodic current in the CVs (Figure 1). However, we subsequently demonstrated that the anodic current is not only not first order with respect to water, the maximum anodic peak current is essentially zero order with respect to water over a ∼550-fold range of water concentration (ranging from 0.018% background water in the zero added water conditions to 10 vol

https://doi.org/10.1021/acssuschemeng.1c01315
ACS Sustainable Chem. Eng. 2021, 9, 10453−10467

Scheme 4. Electrochemical Mechanisms Considered for the Formation of Hypervalent Iodine Species via Anodic Oxidation at a Glassy Carbon Electrode

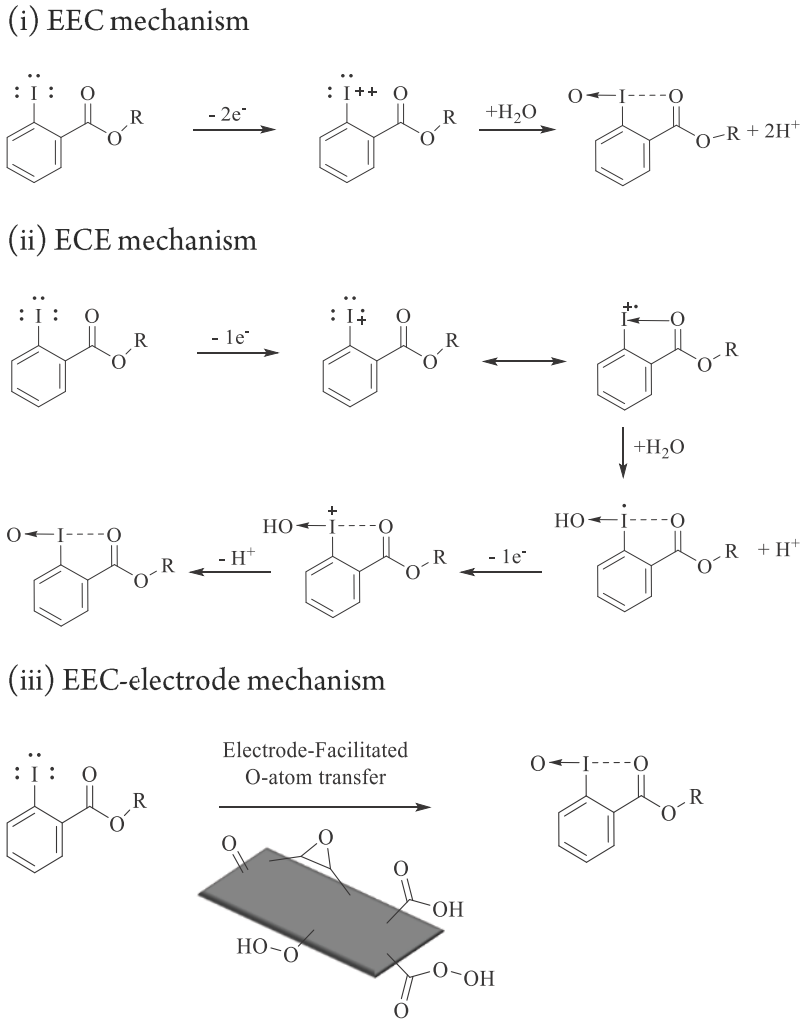

% water; Figures 1 and 7 as well as Figure S2 in the Supporting Information). It is possible that mechanism (i) or (ii) proceeds through a fast electron transfer and is followed by a slow chemical step involving water, but water is not involved in the current-limiting step: evidence against mechanisms (i) and (ii) but not sufficient evidence to disprove them.

However, a second, telling test of the mechanisms in Scheme 4 is that mechanisms (i) and (ii) predict that the use of $H_2{}^{18}O$ should result in the incorporation of ^{18}O atoms into the product, whereas mechanism (iii) can show little to no ^{18}O incorporation at least in the initial product if the native surface-O species on the glassy carbon are not isotopically enriched. Hence, bulk electrolysis was conducted using 97 atom % ^{18}O-enriched $H_2{}^{18}O$.

$PhICO_2Et$ was chosen as the model substrate because the product, IBA-ester, is soluble and stable enough such that it can be analyzed via ESI-MS (while IBA is insoluble and both IBA-sulfone and the IBA/IBX-sulfonic acid mixtures are too reactive/unstable for EIS-MS). For the isotopic experiments, bulk electrolysis was conducted using a freshly cleaned glassy carbon electrode in a standard 20 mL working solution with 20 mM $PhICO_2H$, and 0.1 M $LiClO_4$ in MeCN with 1% added water (v/v) that was, 97 atom % ^{18}O and gave to a final 95 atom % ^{18}O when accounting for water that was already present in the MeCN/$LiClO_4$ solution. The reaction solutions with the MeCN/$LiClO_4$, $PhICO_2Et$, and 1% added water were mixed prior to electrolysis, meaning that the 95 atom % $^{18}OH_2$ was present in solution throughout the entirety of the anodic oxidations.

When conducting electrolysis in this manner, a peak at +293 m/z is observed, consistent with the nonisotopically enriched IBA-ester, $C_9H_8I^{16}O_3{}^+$. Importantly, the +295 peak for $C_9H_8I^{16}O_2{}^{18}O^+$ was either not observed or was observed at a relative intensity (i.e., $C_9H_8I^{16}O_2{}^{18}O^+$ vs $C_9H_8I^{16}O_3{}^+$) that was always <20% and certainly ≪95% as expected if the mechanism consisted of solution-based nucleophilic quenching by water. Furthermore, to disprove solution-based ligand exchange of the water atom, we dissolved $C_9H_8I^{16}O_3{}^+$ in a MeCN solution containing 0.1 M $LiClO_4$ and 1% water (95 atom % ^{18}O) (i.e., the same constitution as the electrolysis solutions) and stirred the solution for 24 h before isolation of the material. No incorporation of ^{18}O was observed from the material isolated from the ligand exchange solution. This observation is consistent with previous studies where ^{16}O and ^{18}O atoms of PhIO are not exchanged in aqueous solutions, and the ligand exchange can only occur through the iodobenzene dimethoxide intermediate synthesized in anhydrous conditions.[47] Furthermore, IBA-ester is stabilized

https://doi.org/10.1021/acssuschemeng.1c01315
ACS Sustainable Chem. Eng. 2021, 9, 10453−10467

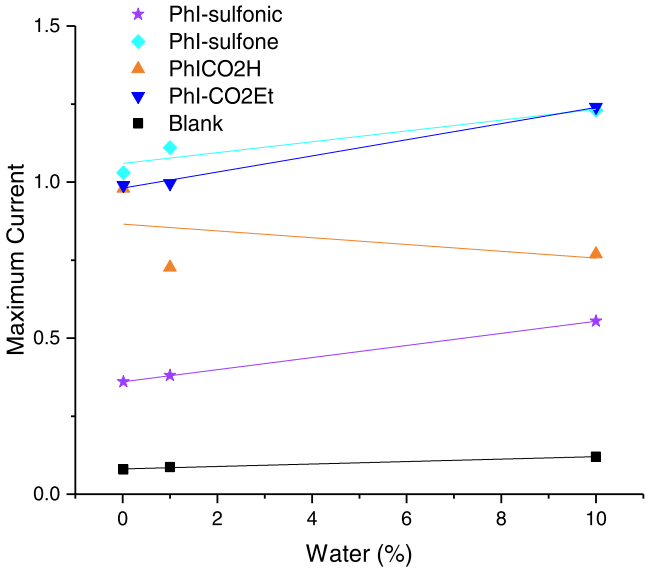

Figure 7. Plot of maximum anodic current vs the amount of water in solution (%) for all of the PhIR compounds and in the absence of added PhIR (blank). None of the maximum currents exhibit more than a ~0.05 power — and hence effectively zero-order — dependence on added water over the ~550-fold range of added water (i.e., over and above the ~0.018% background water present).

through an intramolecular bond and any direct ligand exchange would most likely proceed through nucleophilic attack by water but the backside position is sterically hindered by the ethyl ester group.

If the reaction were to proceed through mechanism (i) or (ii), then incorporation of ^{18}O into the product should match the solution amount of 95 atom % which it does not! Hence, these experiments disprove both the (i) EEC and (ii) ECE mechanisms. They instead support the EEC-electrode mechanism where the O-atoms incorporated into the hypervalent iodine products originate from the surface sites containing transferable O atoms of the glassy carbon—not what we had originally hypothesized. However, it is not surprising that the glassy carbon electrode is able to transfer an O-atom given that its surface of glassy carbon has a variety of O-containing functional groups such as carboxyls, peroxides, quinones, etc.[46]

We further checked the predictions of the EEC-electrode mechanism (iii) with the following series of three labeling experiments. If the EEC-electrode mechanism is correct, then ^{18}O incorporation into the product should increase with time during the reaction as a greater portion of the "active sites" on glassy carbon have time to become regenerated with ^{18}O (Scheme 5). This hypothesis is consistent with small, <20 atom % being observed in other $H_2{}^{18}O$ labeling experiments conducted, where $^{18}OH_2$ was present in 95 atom % prior to and during the anodic oxidation.

To test this hypothesis and mechanism (iii) further, three consecutive electrolyses were conducted in which the same glassy carbon electrode was used without cleaning between the reactions (so as to preserve the surface oxide formed during the previous electrolysis). Each experiment used a fresh solution containing 20 mM $PhICO_2H$, and 0.1 M $LiClO_4$ in MeCN with 1% water (v/v) that was 95 atom % ^{18}O and the

Scheme 5. Glassy Carbon-Mediated O-Atom Transfer and Solution-Based Regeneration of Active Sites Yielding a Small Amount of ^{18}O-Incorporated Product[a]

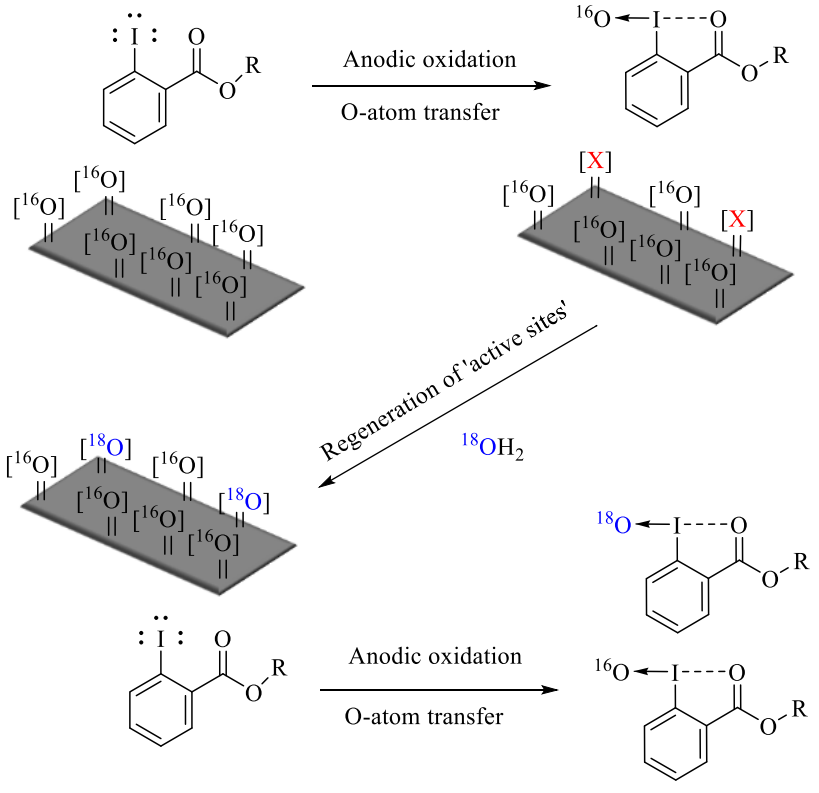

[a]The red Xs represent vacancies on the glassy carbon active sites.

https://doi.org/10.1021/acssuschemeng.1c01315
ACS Sustainable Chem. Eng. 2021, 9, 10453−10467

Table 1. Consecutive Electrolyses Using ^{18}O in Solution and the Percentage of ^{18}O Incorporation into the Hypervalent Iodine Product[a]

electrolysis number	^{18}O IBA-ester ^{16}O IBA-ester (%)
1	9.7
2	14.3
3	17.8

[a]The known $^{18}O/^{16}O$ ratio in solution was 95:5.

electrode was immersed in the premixed solution prior to electrolysis. The results of that experiment are shown in Table 1 where the ratio of $C_9H_8I^{16}O_2{}^{18}O^+$ vs $C_9H_8I^{16}O_3{}^+$ increases with each consecutive experiment, consistent with our hypothesis that glassy carbon "active sites" can be regenerated from solution-based water. This additional ^{18}O labeling experiment provides further evidence consistent with, supportive of—and in fact predicted by—the EEC-electrode mechanism. These results also portend the need to understand better—ideally before attempting scale-up and optimization studies—the rate laws, elementary steps, and their rate constants for carbon-surface-O to PhI-based substrate O-atom transfer, then carbon-surface-[vacancy] + H_2O to regenerate the carbon-surface-O.

It is known that glassy carbon has a native oxide layer, which can affect the observed electrochemical performance.[46] It is also known that under anodic conditions, glassy carbon can decompose into CO_2[48] or other polyaromatic hydrocarbons,[49] and that the surface of glassy carbon can be functionalized using these vacancies.[50] However, to our knowledge (including a SciFinder, Google Scholar, and Web of Science searches of "carbon electrode oxygenations," "oxidation of organics involving water," and "glassy carbon functionalization" among others), the present work is a rare and apparently the first example of glassy carbon-mediated O-atom transfer where glassy carbon selectively oxidizes a solution-based molecule *and then the carbon anode active sites are regenerated from solution-based water*. While we do not, at present, know the precise nature or identity of the carbon anode active sites, the present study likely has more general implications for electrocatalytic reactions using glassy carbon electrodes under anodic conditions as well as for electrosyntheses of hypervalent iodine and other such compounds.

CONCLUSIONS

The electrochemical oxidations of $PhICO_2H$, $PhICO_2Et$, PhI-sulfone, and PhI-sulfonic acid in the absence, and then presence, of added H_2O, have been investigated. Characterization (^1H and ^{13}C NMR, FT-IR, and mass spectrometry where relevant) of the products obtained from bulk electrolysis at 1.8 V of $PhICO_2H$, $PhICO_2Et$, PhI-sulfone, and PhI-sulfonic acid in the presence of added water yields the well-known hypervalent iodine reagents IBA (89% Faradaic efficiency) in up to 58% isolated yield, as novel IBA derivative, IBA-ester (~78% Faradaic efficiency), IBX-sulfone (~51% Faradaic efficiency), and a mixture of IBA /IBX-sulfonic acid (>78% Faradaic efficiency). IBA-ester has been previously inaccessible because the known chemical routes would hydrolyze the ester (Scheme 2); hence, a new electrochemical synthetic route to hypervalent iodine reagents has been demonstrated.

Initial investigations of the electrochemical mechanism of formation revealed that native oxide functionality of glassy carbon directly transfers an O-atom to the hypervalent species in solution. The surface oxide of the glassy carbon is then regenerated using the O-atoms from solution as demonstrated using $H_2{}^{18}O$ labeling studies. Thus, although the initial incorporation of solution-based water molecules is low, in the limit of prolonged oxidation, the bulk of the O-atoms incorporated into the product increasingly come from water. The results are a proof of principle of oxygenation reactions or PhI-based reagents to hypervalent iodine species using water as an abundant, green chemistry O-atom source. The mechanistic studies herein allow future opportunities to scale up and optimize reaction conditions as the electrochemical mechanism is crucial for rational optimization.

In terms of electrocatalysis, there is much to be explored. IBA is known to perform direct O-atom transfer to α,β-unsaturated ketones without an added transition-metal catalysts;[12] it is also a precursor to other group-transfer reagents.[15] Preliminary results with IBA-ester show that it is capable of performing O-atom transfer to PPh_3 without added catalyst. Additionally, both IBX-sulfone and IBA/IBX-sulfonic acid can be used for the oxidation of alcohols, or epoxidation reactions with a transition-metal catalyst.[11,27,28,44] Although IBX-sulfonic was not isolated in this manuscript, one would likely not isolate the O-atom mediator in these cases and would instead be used directly for oxygenation, ideally in a yet-to-be-realized electrocatalytic manner.

Overall, this work provides a proof of principle precedent for the required first step toward the use of hypervalent iodine reagents such as $PhICO_2H$, $PhICO_2Et$, and PhI-sulfone/sulfonic acid as O-atom-transfer mediators for coupling (photo)electrocatalytic water splitting to oxygenation and oxidation reactions yielding value-added products. The synthesis and use of hypervalent iodine reagents in electrocatalytic oxidation and oxygenation reactions conforms to at least three of the principles of green chemistry including: (i) use of a catalytic reagent (Ar-I) rather than a stoichiometric oxidant such as bleach or oxone; (ii) atom economy, using the O-atom from water when producing H_2 and an oxygenated product; and (iii) less hazardous chemical synthesis/inherently safer chemistry—there are reports of explosions during the synthesis of hypervalent iodine reagents;[37] however, using electrocatalytic methods, the hypervalent iodine can at least in principle be used catalytically. Future work will develop the use of Ar-I reagents for electrocatalytic oxygenations and oxidations using water as the O-atom source and (photo)-electrochemistry as the driving force of the reaction. In addition, we will report on the electrochemical synthesis of hypervalent iodine species at a Pt electrode and some interesting findings there.

ASSOCIATED CONTENT

Supporting Information

The Supporting Information is available free of charge at https://pubs.acs.org/doi/10.1021/acssuschemeng.1c01315.

Synthesis of PhI-sulfone following literature methods; calculation of theoretical conversions and Faradaic efficiency determined by ^1H NMR; picture of U-cell used for bulk electrolysis of hypervalent iodine derivatives (Figure S1); full-size cyclic voltammograms from top to bottom of $PhICO_2H$, $PhICO_2Et$, PhI-sulfone, and PhI-sulfonic acid (Figure S2); background CVs of the 0.1 M $LiClO_4$ MeCN solution, with no added water, 1% and 10% added water (Figure S3);

https://doi.org/10.1021/acssuschemeng.1c01315
ACS Sustainable Chem. Eng. 2021, 9, 10453−10467

picture of U-cell during bulk electrolysis of $PhICO_2H$ at 50% conversion (Figure S4); full-size Figure 3 from the main text (Figure S5); ^{13}C NMR of $PhICO_2H$, IBX, IBA, and precipitate isolated from the bulk electrolysis of $PhICO_2H$; all of the ^{13}C NMR peaks of the isolated material are consistent with the formation of λ^3-IBA and not λ^5-IBX (Figure S6); FT-IR spectra of authentic $PhICO_2H$, IBA, and electrochemically synthesized IBA (Figure S7); qNMR plot of the normalized peak integration of the post electrolysis, 250 mL scale-up reaction, spiked with authentic IBA (Figure S8); full-size Figure 4 from the main text (Figure S9); ^{13}C NMR of $PhICO_2Et$, IBX-ester, and isolated IBA-ester (Figure S10); mass spectrum of isolated $PhICO_2Et$ (blue) and electrochemically synthesized IBA-ester (red) (Figure S11); FT-IR spectra of $PhICO_2Et$ and the isolated IBA-ester after 77 C of electrolysis (Figure S12); FT-IR spectra of the isolated IBA-ester and compared with the free acid IBA (Figure S13); full-size Figure 5 from the main text (Figure S14); full-size Figure 6 from the main text (Figure S15); and product, isolated yield, and Faradaic efficiency and PhIR electrolyses (Table S1) (PDF)

AUTHOR INFORMATION

Corresponding Authors

Scott J. Folkman − *Chemistry Department, Colorado State University, Fort Collins, Colorado 80521, United States; Institute of Chemical Research of Catalonia (ICIQ), The Barcelona Institute of Science and Technology, 43007 Tarragona, Spain*; Email: sfolkman@iciq.es

Garret M. Miyake − *Chemistry Department, Colorado State University, Fort Collins, Colorado 80521, United States;* orcid.org/0000-0003-2451-7090; Email: garret.miyake@colostate.edu

Authors

Richard G. Finke − *Chemistry Department, Colorado State University, Fort Collins, Colorado 80521, United States;* orcid.org/0000-0002-3668-7903

José Ramón Galán-Mascarós − *Institute of Chemical Research of Catalonia (ICIQ), The Barcelona Institute of Science and Technology, 43007 Tarragona, Spain; ICREA, 08010 Barcelona, Spain;* orcid.org/0000-0001-7983-9762

Complete contact information is available at: https://pubs.acs.org/10.1021/acssuschemeng.1c01315

Notes

The authors declare no competing financial interest.

ACKNOWLEDGMENTS

This work was supported by the National Institutes of Health under Award Number R35GM119702. S.J.F. acknowledges Marie Skłodowska-Curie Actions grant agreement 895296 (IF-2019). R.G.F.'s time was supported by NSF grant No. 1664646. The authors also acknowledge the thorough and insightful feedback received from the reviewers.

REFERENCES

(1) Bard, A. J.; Fox, M. A. Artificial Photosynthesis: Solar Splitting of Water to Hydrogen and Oxygen. *Acc. Chem. Res.* **1995**, *28*, 141−145.

(2) Li, T.; Kasahara, T.; He, J.; Dettelbach, K. E.; Sammis, G. M.; Berlinguette, C. P. Photoelectrochemical Oxidation of Organic Substrates in Organic Media. *Nat. Commun.* **2017**, *8*, No. 390.

(3) Zhang, P.; Sheng, X.; Chen, X.; Fang, Z.; Jiang, J.; Wang, M.; Li, F.; Fan, L.; Ren, Y.; Zhang, B.; et al. Paired Electrocatalytic Oxygenation and Hydrogenation of Organic Substrates with Water as the Oxygen and Hydrogen Source. *Angew. Chem., Int. Ed.* **2019**, *58*, 9155−9159.

(4) Reid, L. M.; Li, T.; Cao, Y.; Berlinguette, C. P. Organic Chemistry at Anodes and Photoanodes. *Sustainable Energy Fuels* **2018**, *2*, 1905−1927.

(5) Maalouf, J. H.; Jin, K.; Yang, D.; Limaye, A. M.; Manthiram, K. Kinetic Analysis of Electrochemical Lactonization of Ketones Using Water as the Oxygen Atom Source. *ACS Catal.* **2020**, *10*, 5750−5756.

(6) Jin, K.; Maalouf, J. H.; Lazouski, N.; Corbin, N.; Yang, D.; Manthiram, K. Epoxidation of Cyclooctene Using Water as the Oxygen Atom Source at Manganese Oxide Electrocatalysts. *J. Am. Chem. Soc.* **2019**, *141*, 6413−6418.

(7) Leow, W. R.; Lum, Y.; Ozden, A.; Wang, Y.; Nam, D.; Chen, B.; et al. Chloride-Mediated Selective Electrosynthesis of Ethylene and Propylene Oxides at High Current Density. *Science* **2020**, *368*, 1228−1233.

(8) Groves, J. T.; Kruper, W. J.; Nemo, T. E.; Myers, R. S. Hydroxylation and Expoxidation Reactions Catalyzed by Synthetic Metalloporphyrinates. Models Related to the Active Oxygen Species of Cytochrome P-450. *J. Mol. Catal.* **1980**, *7*, 169−177.

(9) Protasiewicz, J. D. Organoiodine(III) Reagents as Active Participants and Ligands in Transition Metal-Catalyzed Reactions: Iodosylarenes and (Imino)iodoarenes. In *HyperValent Iodine Chemistry*; With, T., Ed.; Springer International: Switzerland, 2015; pp 263−288.

(10) Dohi, T.; Kita, Y. Hypervalent Iodine Reagents as a New Entrance to Organocatalysts. *Chem. Commun.* **2009**, 2073−2085.

(11) Yusubov, M. S.; Nemykin, V. N.; Zhdankin, V. V. Transition Metal-Mediated Oxidations Utilizing Monomeric Iodosyl- and Iodylarene Species. *Tetrahedron* **2010**, *66*, 5745−5752.

(12) Ochiai, M.; Nakanishi, A.; Suefuji, T. Unprecedented Direct Oxygen Atom Transfer from Hypervalent Oxido-λ^3-Iodanes to α,β-Unsaturated Carbonyl Compounds: Synthesis of α,β-Epoxy Carbonyl Compounds. *Org. Lett.* **2000**, *2*, 2923−2926.

(13) Mahoney, W. C.; Hermodson, M. A. High-Yield Cleavage of Tryptophanyl Peptide Bonds by o-Iodosobenzoic Acid. *Biochemistry* **1979**, *18*, 3810−3814.

(14) Fontana, A.; Dalzoppo, D.; Grandi, C.; Zambonin, M. Cleavage at Tryptophan with o-Iodosobenzoic Acid. In *Methods in Enzymology*; Enzyme Structure Part I; Academic Press, 1983; Vol. *91*, pp 311−318.

(15) Li, Y.; Hari, D. P.; Vita, M. V.; Waser, J. Cyclic Hypervalent Iodine Reagents for Atom-Transfer Reactions: Beyond Trifluoromethylation. *Angew. Chem., Int. Ed.* **2016**, *55*, 4436−4454.

(16) Eisenberger, P.; Gischig, S.; Togni, A. Novel 10-I-3 Hypervalent Iodine-Based Compounds for Electrophilic Trifluoromethylation. *Chem. - Eur. J.* **2006**, *12*, 2579−2586.

(17) Zhdankin, V. V.; Krasutsky, A. P.; Kuehl, C. J.; Simonsen, A. J.; Woodward, J. K.; Mismash, B.; Bolz, J. T. Preparation, X-Ray Crystal Structure, and Chemistry of Stable Azidoiodinanes-Derivatives of Benziodoxole. *J. Am. Chem. Soc.* **1996**, *118*, 5192−5197.

(18) Ivanov, A. S.; Popov, I. A.; Boldyrev, A. I.; Zhdankin, V. V. The I = X (X = O,N,C) Double Bond in Hypervalent Iodine Compounds: Is It Real? *Angew. Chem., Int. Ed.* **2014**, *53*, 9617−9621.

(19) Bystron, T.; Horbenko, A.; Syslova, K.; Hii, K. K. M.; Hellgardt, K.; Kelsall, G. 2-Iodoxybenzoic Acid Synthesis by Oxidation of 2-Iodobenzoic Acid at a Boron-Doped Diamond Anode. *ChemElectroChem* **2018**, *5*, 1002−1005.

(20) Devadas, B.; Svoboda, J.; Krupička, M.; Bystron, T. Electrochemical and Spectroscopic Study of 2-Iodobenzoic Acid and 2-Iodosobenzoic Acid Anodic Oxidation in Aqueous Environment. *Electrochim. Acta* **2020**, *342*, No. 136080.

(21) Fuchigami, T.; Fujita, T. Electrolytic Partial Fluorination of Organic Compounds. 14. The First Electrosynthesis of Hypervalent

Iodobenzene Difluoride Derivatives and Its Application to Indirect Anodic Gem-Difluorination. *J. Org. Chem* **1994**, *59*, 7190−7192.
(22) Elsherbini, M.; Wirth, T. Hypervalent Iodine Reagents by Anodic Oxidation: A Powerful Green Synthesis. *Chem. - Eur. J.* **2018**, *24*, 13399−13407.
(23) Francke, R. Electrogenerated Hypervalent Iodine Compounds as Mediators in Organic Synthesis. *Curr. Opin. Electrochem.* **2019**, *15*, 83−88.
(24) Maity, A.; Frey, B. L.; Hoskinson, N. D.; Powers, D. C. Electrocatalytic C−N Coupling via Anodically Generated Hypervalent Iodine Intermediates. *J. Am. Chem. Soc.* **2020**, *142*, 4990−4995.
(25) Roesel, A. F.; Broese, T.; Májek, M.; Francke, R. Iodophenylsulfonates and Iodobenzoates as Redox-Active Supporting Electrolytes for Electrosynthesis. *ChemElectroChem* **2019**, *6*, 4229−4237.
(26) Zu, B.; Ke, J.; Guo, Y.; He, C. Synthesis of Diverse Aryliodine(III) Reagents by Anodic Oxidation. *Chin. J. Chem.* **2021**, *39*, 627−632.
(27) Koposov, A. Y.; Litvinov, D. N.; Zhdankin, V. V.; Ferguson, M. J.; McDonald, R.; Tykwinski, R. R. Preparation and Reductive Decomposition of 2-Iodoxybenzenesulfonic Acid. X-Ray Crystal Structure of 1-Hydroxy-1H-1,2,3-Benziodoxathiole 3,3-Dioxide. *Eur. J. Org. Chem.* **2006**, 4791−4795.
(28) Uyanik, M.; Akakura, M.; Ishihara, K. 2-Iodoxybenzenesulfonic Acid As an Extremely Active Catalyst for the Selective Oxidation of Alcohols To Aldehydes, Ketones, Carboxylic Acids, and Enones With Oxone. *J. Am. Chem. Soc.* **2009**, *131*, 251−262.
(29) Kraszkiewicz, L.; Skulski, L. Optimized Syntheses of Iodylarenes from Iodoarenes, with Sodium Periodateas the Oxidant. Part II. *Arkivoc* **2003**, *2003*, 120−125.
(30) Zhdankin, V. V. Hypervalent iodine(III) Reagents in Organic Synthesis. *ARKIVOC* **2009**, *2009*, 1−62.
(31) Macikenas, D.; Skrzypczak-Jankun, E.; Protasiewicz, J. D. A New Class of Iodonium Ylides Engineered as Soluble Primary Oxo and Nitrene Sources. *J. Am. Chem. Soc.* **1999**, *121*, 7164−7165.
(32) Miyamoto, K.; Yamashita, J.; Narita, S.; Sakai, Y.; Hirano, K.; Saito, T.; Wang, C.; Ochiai, M.; Uchiyama, M. Iodoarene-Catalyzed Oxidative Transformations Using Molecular Oxygen. *Chem. Commun.* **2017**, *53*, 9781−9784.
(33) Maity, A.; Hyun, S. M.; Powers, D. C. Oxidase Catalysis via Aerobically Generated Hypervalent Iodine Intermediates. *Nat. Chem.* **2018**, *10*, 200−204.
(34) Cardenal, A. D.; Maity, A.; Gao, W. Y.; Ashirov, R.; Hyun, S. M.; Powers, D. C. Iodosylbenzene Coordination Chemistry Relevant to Metal-Organic Framework Catalysis. *Inorg. Chem.* **2019**, *58*, 10543−10553.
(35) Zhdankin, V. V.; Protasiewicz, J. D. Development of New Hypervalent Iodine Reagents with Improved Properties and Reactivity by Redirecting Secondary Bonds at Iodine Center. *Coord. Chem. Rev.* **2014**, *275*, 54−62.
(36) Rundlöf, T.; Mathiasson, M.; Bekiroglu, S.; Hakkarainen, B.; Bowden, T.; Arvidsson, T. Survey and Qualification of Internal Standards for Quantification by 1H NMR Spectroscopy. *J. Pharm. Biomed. Anal.* **2010**, *52*, 645−651.
(37) Plumb, J. B.; Harper, D. 2-Iodoxybenzoic Acid. *Chem. Eng. News* **1990**, *68*, 23−45.
(38) Frigerio, M.; Santagostino, M.; Sputore, S. A User-Friendly Entry to 2-Iodoxybenzoic Acid (IBX). *J. Org. Chem* **1999**, *64*, 4537−4538.
(39) Matsui, T.; Kitagawa, Y.; Okumura, M.; Shigeta, Y. Accurate Standard Hydrogen Electrode Potential and Applications to the Redox Potentials of Vitamin C and NAD/NADH. *J. Phys. Chem. A* **2015**, *119*, 369−376.
(40) Laue, S.; Haverkamp, V.; Mleczko, L. Experience with Scale-Up of Low-Temperature Organometallic Reactions in Continuous Flow. *Org. Process Res. Dev.* **2016**, *20*, 480−486.
(41) Szpyrkowicz, L.; Radaelli, M. Scale-up of an Electrochemical Reactor for Treatment of Industrial Wastewater with an Electrochemically Generated Redox Mediator. *J. Appl. Electrochem.* **2006**, *36*, 1151−1156.
(42) Katritzky, A. R.; Gallos, J. K.; Durst, H. D. Structure of and Electronic Interactions in Aromatic Polyvalent Iodine Compounds: A ^{13}C NMR Study. *Magn. Reson. Chem.* **1989**, *27*, 815−822.
(43) Zhdankin, V. V.; Kuehl, C. J.; Krasutsky, A. P.; Bolz, J. T.; Simonsen, A. J. 1-(Organosulfonyloxy)-3(1H)-1,2-Benziodoxoles: Preparation and Reactions with Alkynyltrimethylsilanes. *J. Org. Chem.* **1996**, *61*, 6547−6551.
(44) Mironova, I. A.; Postnikov, P. S.; Yusubova, R. Y.; Yoshimura, A.; Wirth, T.; Zhdankin, V. V.; Nemykin, V. N.; Yusubov, M. S. Preparation and X-Ray Structure of 2-Iodoxybenzenesulfonic Acid (IBS) − A Powerful Hypervalent iodine(V) Oxidant. *Beilstein J. Org. Chem.* **2018**, *14*, 1854−1858.
(45) Andrieux, C. Terminology and Notations for Multistep Electrochemical Reaction Mechanisms. *Pure Appl. Chem.* **1994**, *66*, 2445−2450.
(46) Kamau, G. N. Surface Preparation of Glassy Carbon Electrodes. *Anal. Chim. Acta* **1988**, *207*, 1−16.
(47) Schardt, B. C.; Hill, C. L. Preparation of Iodobenzene Dimethoxide. A New Synthesis of [18O]Iodosylbenzene and a Reexamination of Its Infrared Spectrum. *Inorg. Chem.* **1983**, *22*, 1563−1565.
(48) Ullman, A. M.; Liu, Y.; Huynh, M.; Bediako, D. K.; Wang, H.; Anderson, B. L.; Powers, D. C.; Breen, J. J.; Abruña, H. D.; Nocera, D. G. Water Oxidation Catalysis by Co(II) Impurities in Co(III)4O4 Cubanes. *J. Am. Chem. Soc.* **2014**, *136*, 17681−17688.
(49) Yi, Y.; Weinberg, G.; Prenzel, M.; Greiner, M.; Heumann, S.; Becker, S.; Schlögl, R. Electrochemical Corrosion of a Glassy Carbon Electrode. *Catal. Today* **2017**, *295*, 32−40.
(50) Hernández, D. M.; González, M. A.; Astudillo, P. D.; Hernández, L. S.; González, F. J. Modification of Carbon Electrodes by Anodic Oxidation of Organic Anions. *Procedia Chem.* **2014**, *12*, 3−8.

https://doi.org/10.1021/acssuschemeng.1c01315
ACS Sustainable Chem. Eng. 2021, 9, 10453−10467